Proceedings of the 2009 IEEE International Conference on Systems, Man, and Cybernetics
San Antonio, TX, USA - October 2009

Path Loss Revisited Using Computer Simulation

Hung Huy Khong, Bing W. Kwan, Leonard J. Tung
Department of Electrical & Computer Engineering, FAMU-FSU College of Engineering
Florida State University, Tallahassee, FL, 32310
Email: {khonghu, kwan, tung}@eng.fsu.edu

***Abstract*— In this paper, we propose a computer simulation model for the study of the large-scale effects on narrowband wireless transmission systems. The development of the path loss model is based on the ray tracing technique. This study concentrates on the first-order scattering effects, namely each multipath signal is a two-hop signal that involves a single scattering object. The first hop is directed toward the scatterer from the transmitter; and the second hop goes from the scatterer to the receiver. For each hop the signal is described using a two-ray model accounting for wave propagation along the direct path and along the ground-reflected path. The simulation results are consistent with the empirical models that are derived from measurements, including the Hata model and the Lee model. More importantly, two key observations are made: First, the path loss is affected by the number of scattering objects, their radar cross sections, and the ground reflection. Second, coherent multipath signals can cause the path-loss exponent falling below 2, which corresponds to free-space propagation.**

***Keywords*— narrowband, path loss, ray tracing.**

I. INTRODUCTION

It is desirable to ensure that the data transmission between the transmitter (TX) and the receiver (RX) is as reliable as possible. This means understanding the channel characteristics is critical in the design and optimization of a communication system. Before designing a wireless communication system, the received signal level or path loss needs to be investigated carefully. Most radio signal propagation models are derived using empirical methods which are based on fitting mathematical models to measurement data.

Many research efforts have been devoted to modeling the propagation effects – especially path loss – using different methods ranging from analytical models, semi-empirical models, to empirical models. In particular, numerous measurement-based narrowband path-loss models have been proposed and investigated. The path loss for macro cells with coverage area having radius from 1 km to 20 km has been proposed by Hata, Lee, and several other research groups [1], [2], [3]. These models will be used as reference for comparison with the computer simulation results obtained using the model proposed in this study. The path loss models based on measurement data for micro-cell areas were also investigated and documented [3]. These research works were generally tedious and costly because specialized expensive equipment was involved.

The two-ray models using the ray tracing technique, which is based on geometrical optics, are most commonly used to predict the path loss [4], [5]. This technique assumes a finite number of multipath signals from the TX to the RX. Further, the knowledge about the physical elements of the channel is essential, including the geometry of the scattering objects in the channel. To simplify the solution procedure, however, the ray tracing technique often makes approximation to obtain the excess path length. Typically, it is assumed that the distance between the receiver and the nearest scattering object is many wavelengths and the scattering objects are electrically large compared to the wavelength [6]-[8]. Several research efforts reported in the literature [9], [10] have employed the ray tracing technique.

This paper will develop a model based on the ray tracing technique that is particularly suitable for computer simulations. The proposed model is applicable to an arbitrary number of scattering objects. The wave (signal) interactions between the TX, the scattering objects and the RX are based on the two-ray model without making restrictive assumptions. The two-ray model considers the effects of direct-path wave propagation and the ground-reflected path wave propagation. In addition, the proposed model allows the flexibility in studying the dependence of path loss on the density of scattering objects, the distance between the TX and the RX, the radar cross sections, and the ground reflection. In particular, the research work found in [11]-[13] provides the basis of this study.

This paper is organized as follows: section II discusses the commonly used empirical models for predicting path loss, which include the Hata model and the Lee model. A path loss model based on the ray tracing technique is introduced in section III. The computer simulation results and key findings are discussed in section IV. Comparisons with the popular empirical models are also made. Finally, section V concludes the paper.

II. PATH LOSS MODELING

A. Line-of-Sight Wave Propagation

The model for path loss associated with wave propagating along the line of sight (LOS) is straightforward. The received power P_r is related to the transmitted power P_t via the Friis transmission formula [7]:

$$P_r = \frac{EIRP}{4\pi d^2} A_e = \frac{P_t G_t G_r \lambda^2}{(4\pi d)^2} \quad (1)$$

In (1), EIRP stands for the equivalent isotropic radiated power defined by the product $P_t G_t$. The transmitting antenna has gain G_t while the receiving antenna has gain G_r. Distance d is the separation between the TX and the RX. The RX has an

effective aperture given by $A_e = G_r\lambda^2/4\pi$, where λ is the signal wavelength. The path loss is defined as

$$P_L(d) \equiv \frac{P_r}{P_t G_t G_r} = \left(\frac{\lambda}{4\pi d}\right)^2 = \frac{A_e}{4\pi G_r d^2} \qquad (2)$$

B. Non-LOS Wave Propagation

Since there are scattering objects in the channel, it is quite likely that the transmitted signal cannot reach the RX directly as the LOS path is blocked. Unlike the LOS case, the modeling of path loss in the non-line-of-sight (NLOS) environment is more complex. The parameters of many physical elements affecting wave propagation are involved. A popular NLOS path loss model is semi-empirical and assumes the form [7]:

$$P_L(d) = P_L(d_0) + 10n\log_{10}\left(\frac{d}{d_0}\right) + S(d) \quad [\text{dB}] \qquad (3)$$

In (3), $P_L(d_0)$ is the path loss at a reference distance d_0 from the TX; $S(d)$ accounts for the lognormal shadow fading effects; and n is the path loss exponent. Many experiments and results have been reported for both LOS and NLOS environments, covering the frequency range from 100 MHz to 2 GHz, which is the frequency band for most narrowband transmission systems. According to (3), the path loss in dB is assumed to be the linear function of log distance (to the base 10) with loss exponent n and intercept $P_L(d_0)$.

C. Empirical Path Loss Model for Macro Cells

Summarized here are the two popular empirical models derived from measurement data taken in macro cellular environment with path distance ranging from 1km to 20km. The models were separately proposed and developed by Hata [1] and Lee [2]. The common characteristic of these models are the linear dependence of path loss on the distance from the TX to the RX as depicted in (3). For the purpose of comparison, the path losses predicted by these models are plotted in Fig. 1. The specific parameter values used in the calculations are as follows: transmitting antenna height $h_t = 70\,\text{m}$, receiving antenna height $h_r = 2\,\text{m}$, and the carrier frequency 900 MHz.

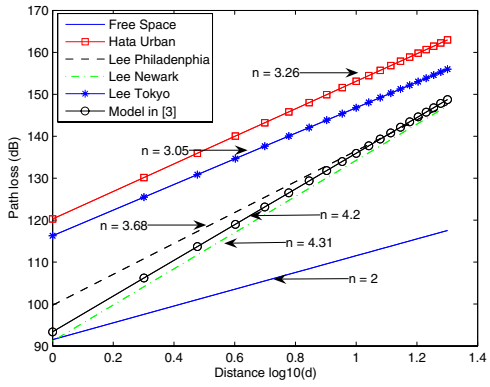

Figure 1. Path losses predicted by the Free space, Hata and Lee models for macro cells

One may observe the path loss exponent predicted by these models varies from 2 to 4 and the intercept value ranges from 90 to 120 dB. These values will serve as reference for the comparison with the path loss model presented in this study.

III. PATH LOSS MODEL BASED ON RAY TRACING TECHNIQUE

In the intervening medium between the TX and the RX, we assume there are numerous scattering objects to characterize the rich NLOS multipath environment. Each scattering object absorbs the direct signal power from the TX along the LOS path coupled with the indirect signal power reflected off the ground. To be specific, consider scattering object i shown in Fig. 2. It is at distance d_1 from the TX along the direct path and distance d_1' along the ground-reflected path. The total power absorbed by the object is then re-radiated omni-directionally. The RX is at distance d_2 along the direct path and distance d_2' along the ground-reflected path. The power absorbed by object i depends on its radar cross section $\sigma_s(i) = \pi R(i)^2$, which is taken to be a circular area with radius $R(i)$. Without loss of generality, it is assumed that the LOS path between the TX and the RX is blocked and is not taken into consideration in this study.

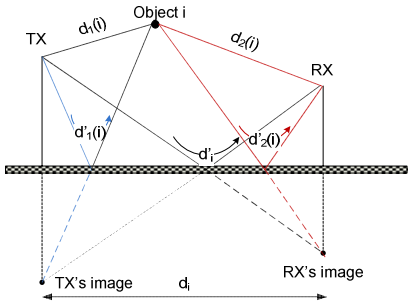

Figure 2. A two-hop multipath signal based on the 2-ray model

The electric field incident upon scattering object i can be expressed in terms of the electric field intensity:

$$E_1(i) = E_0\left(\frac{1}{d_1(i)}e^{-j\beta d_1(i)} + \frac{\Gamma_g}{d_1'(i)}e^{-j\beta d_1'(i)}\right) \qquad (4)$$

In (4), $E_0 = \sqrt{\eta \cdot EIRP/2\pi}$ denotes the electric field amplitude with η = 377 Ω for free space, $\beta = 2\pi/\lambda$ the phase constant, and Γ_g the ground reflection coefficient. The time-average signal power density arriving at the object is given by:

$$S_{object}(i) = \frac{1}{2\eta}E_1^2(i) \qquad (\text{W/m}^2) \qquad (5)$$

In this study, the incident signal power absorbed by object i is treated as the power to be subsequently reradiated. The equivalent isotropic radiated power due to object i is approximated by:

$$EIRP(i) = S_{object}(i) \times \sigma_s(i) = \frac{E_1^2(i) \times \pi R(i)^2}{2\eta} \quad (6)$$

The corresponding power densities along the direct path and the ground-reflected path are respectively computed by:

$$S_{Rx1}(i) = \frac{EIRP(i)}{4\pi d_2(i)^2} = \frac{E_1^2(i) \times \pi R(i)^2}{8\pi\eta d_2(i)^2} \quad (7)$$

$$S_{Rx2}(i) = \frac{EIRP(i)}{4\pi d'_2(i)^2} = \frac{E_1^2(i) \times \pi R(i)^2}{8\pi\eta d'_2(i)^2} \quad (8)$$

The electric field at the receiver due to object i can be expressed as:

$$E_r(i) = \frac{E_1(i)R(i)}{2d_2(i)^2} \times e^{-j\beta d_2(i)} + \Gamma_g \frac{E_1(i)R(i)}{2d'_2(i)^2} \times e^{-j\beta d'_2(i)} \quad (9)$$

In a NLOS environment consisting of N scattering (reflecting) objects, the total electric field at the RX is given by the sum:

$$E_{total} = \sum_{i=1}^{N} E_r(i) \quad (10)$$

The time-average incident signal power density at the receiver is determined by

$$S = \frac{1}{2\eta} E_{total} \cdot E_{total}^* \qquad (\mathrm{W/m^2}) \quad (11)$$

Accordingly the total average power received by the RX may be viewed as the average power intercepted by the receiving antenna with effective aperture A_e and is calculated by

$$P_r = S \cdot A_e = \frac{A_e}{2\eta} |E_{total}|^2 \qquad (\mathrm{W}) \quad (12)$$

To be consistent with the popular semi-empirical models, the path loss in dB is defined as

$$P_L[\mathrm{dB}] = -10 log\left(\frac{P_r}{P_t G_t G_r}\right) \quad (13)$$

It may be readily recognized that P_L does not depend on the EIRP of the TX.

IV. COMPUTER SIMULATIONS

A. Simulation Procedure

To conduct the computer simulations, the intervening medium between the TX and the RX is a 3 dimensional space enclosed by an appropriate Fresnel ellipsoidal surface. The axis of the Fresnel ellipsoid coincides with the y-axis, extending from 0 to s_0 m. The TX is fixed at y = 0, whereas the location of the RX varies from y = 1000 m to y = s_0 m. This choice of the channel space allows the flexibility to study of the effects of scattering objects distributed in different Fresnel zones. In this study, N reflecting objects randomly distributed within a large Fresnel zone are considered. For the computer simulation runs, we set $EIRP = 1$ kW, $f_c = 900$ MHZ, $s_0 = 20$ km. The antenna heights $h_t = 70$m, $h_r = 2$m are used to match the parameters used in measurement studies mentioned previously. The antennas are set to have unity gain, namely $G_t = G_r = 1$. In order to reach statistically meaningful conclusions, 1000 simulation runs are performed for a given number of scattering objects N. A typical simulation run involves three key steps:

Step 1: Set the separation distance d between the TX and the RX, the ground reflection coefficient Γ_g. Select the number of reflecting objects N, and then randomly generate their locations (x_i, y_i, z_i), $i = 1, 2 \ldots, N$, above the earth ground inside the artificial ellipsoid. The radar cross section radii $R(i)$ of these objects are also randomly generated.

Step 2: Compute the electric fields (signals) at the RX according to the model described above.

Step 3: Compute the path loss using equation (13).

B. Path Loss versus Distance

In this section, the dependence of path loss on the separation distance d between the TX and the RX is discussed. To be specific, the radii of the scattering objects vary from 1m to 5m, Γ_g is set at -1 (assuming perfect reflection). The simulation results have been documented in [12] and [13] and are summarized here for the sake of easy reference. Fig. 3 shows the path loss in dB due to 1000 random distributions of 10 scattering objects against log distance. A straight line is used to fit the mean path losses at various log distances with minimum squared errors. This best-fit curve has a loss exponent 0.7 and an intercept 102 dB. The histograms of path losses due to 1000 random distributions of 10, 50, and 150 scattering objects against log distance are also reported. It has been discovered that the path loss exponents cover the range from 2 to 4, while the intercept value varies from 90 dB to 120 dB. These values are in very good agreement with those predicted by the Hata and the Lee models as shown in Fig. 1. Fig. 4 shows the histograms of path-loss exponent and intercept for the case of N = 50 scattering objects. It should be mentioned that the path loss exponent and intercept value depend on the number of scattering objects.

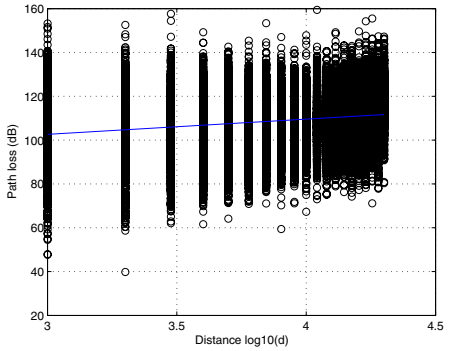

Figure 3. Path loss based on computer simulations for N = 10 objects. The path-loss exponent is 0.7 and intercept is 102 dB.

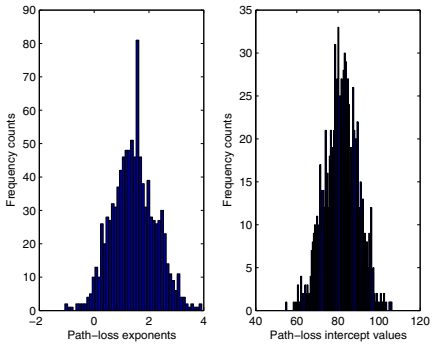

Figure 4. Histograms of path loss exponents and intercept values for $N = 50$ scattering objects

It may occur strikingly surprising that the path-loss exponent can assume negative values, which correspond to the physically unrealizable phenomenon of signals gaining power as they propagate. These negative values in fact stem from the artifical curve-fitting procedure. As pointed out in [12], fitting a straight line through the data points that are randomly correlated may lead to negative slope. This means many simulation runs have resulted in the path losses that are not linearly correlated with log distance, especially when the number of scattering objects is small. In essence, one can argue the lognormal model used to account for the shadowing effect may be more appropriate for dense wireless channels.

C. Key Findings from Computer Simulations

1) Unnatural Path-loss Exponents

From Figure 4 one may notice the unusual result that the path-loss exponents are less than 2, which is the natural free-space path loss exponent. It is in fact only natural to expect the path loss exponent is no less than 2. To seek an explanation for such an unnatural phenomenon, the computer simulation is adjusted to make the signals scattered from the objects arrive at the RX coherently, namely the signals will add in phase. To ensure phase coherence of the multipath signals, the location of scattering object i is so chosen that its distance parameters $d_2(i)$ and $d'_2(i)$ as depicted in Fig. 5 satisfy the condition in (14) subject to the constraint in (15).

$$[d'_2(i) - d_2(i)]\frac{2\pi}{\lambda} = 2p\pi + Y\pi \qquad (14)$$

$$-1 < cos(\alpha) = \frac{d_2^2(i) + (2h_r)^2 - d_2'^2(i)}{4d_2(i)h_r} < 1 \qquad (15)$$

In (14), Y is a random number between 0 to 1, p is a random positive integer number, and the receiving antenna height is h_r in (15). The arriving signals under these conditions will effectively have the same phase $Y\pi$ at the RX. The histogram of the path-loss exponent of coherent signals generated by 1000 simulation runs for $N = 50$ scattering objects is shown in Fig. 6. One may therefore conclude that the unnatural path loss exponent less than 2 is highly likely due to the in-phase addition of the coherent signals arriving at the RX.

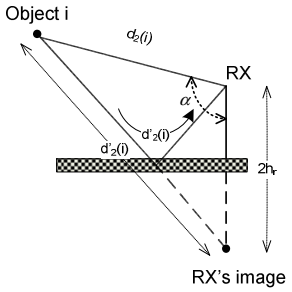

Figure 5. The vertices of the triangle formed by object i, the RX, and the RX's image

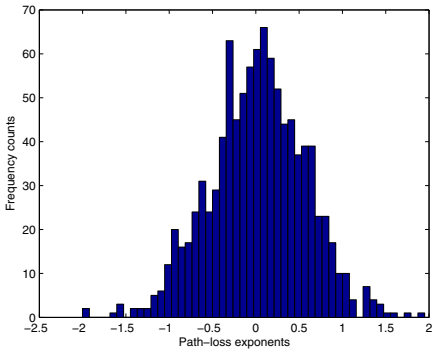

Figure 6. Histograms of path loss exponents and intercept values for $N = 50$ scattering objects for in-phase signals scenario

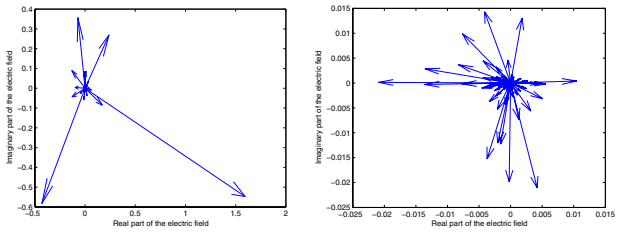

Figure 7. Typical ditribution patterns of electric-field phasors associated with multipath signals received at short distance $d = 1$ km (left) and at long distance $d = 20$ km (right) for $N = 100$ objects

2) Statistical Regularity of Received Signals

It may be noted from Figure 3 that the path loss varies more widely at smaller distances than at larger distances between the TX and the RX. Such a characteristic may be attributed to the manner in which the received signals reach statistical regularity by virtue of the law of large numbers. In the case of small separations, there are fewer dominant received signals scattered by the nearby objects as shown in Figure 7. These dominant signals vary considerably from simulation to simulation, thereby resulting in large variance. In the case of large separations, most objects behave more or less equally as distant scatters, thus producing stationary signals with smaller variance at the receiver. Again Figure 7 depicts such a case with a large

number of statistically similar signals scattered by distant objects.

3) Effect of Scattering Object Size

The amount of incident signal power absorbed by an object and then reradiated as scattered signals can be accounted for by its radar cross section. The radar cross section of an object is taken to be circular in this study for simplicity. The impact of object size on the path loss is studied by running simulations for three groups of objects, each having a different range of radar cross sections characterized by the radii: group 1 with radius R ranging from 1 to 5 m, group 2 with $5 < R < 15$ m, and group 3 with $15 < R < 30$ m. A total of 1000 simulations are run for each group by setting $N = 100$ and $\Gamma_g = -1$.

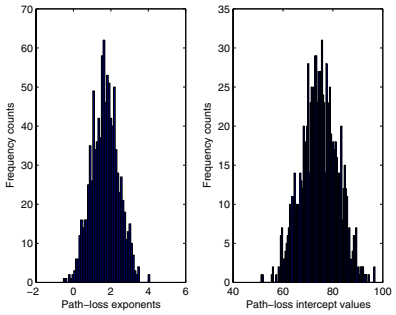

Figure 8. Histograms of path loss exponents and intercept values for $R = 1 - 5$m (mean exponent = 1.7; mean intercept = 75 dB)

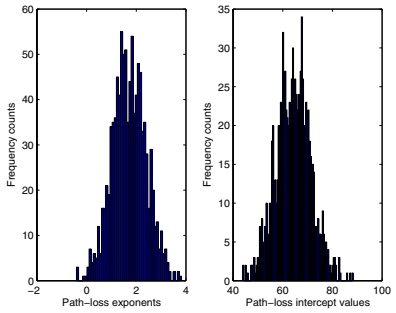

Figure 9. Histograms of path loss exponents and intercept values for $R = 5 - 15$m (mean exponent = 1.7; mean intercept = 65 dB)

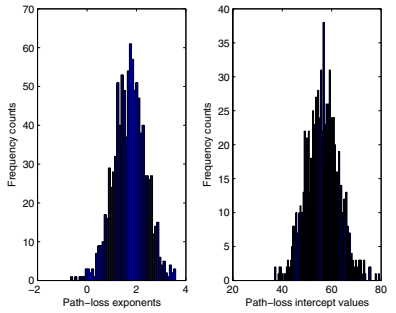

Figure 10. Histograms of path loss exponents and intercept values for $R = 15 - 30$m (mean exponent = 1.7, mean intercept = 56 dB)

The simulation results for group 1 are shown in Fig. 8, which displays the histogram of the path-loss exponents and the histogram of the path-loss intercept values. Similar histograms for group 2 and group 3 are found in Fig. 9 and Fig. 10, respectively. The mean values of the path-loss exponent and intercep for the three groups are listed in Table I.

Clearly, the simulation results are consistent with two facts: First, the spatial rate of signal attenuation remains unchanged regardless of the signal strength. This suggests the path-loss exponent should remain constant. Second, the received signal strength is proportional to the amount of signal power scattered by the objects. This suggests larger scattering objects will result in smaller path loss, hence lower the intercept value.

TABLE I. MEAN PATH LOSS EXPONENTS AND INTERCEPT VALUES FOR THREE DIFFERENT GROUPS OF OBJECTS

Radar Cross Section	Mean Exponent	Mean Intercept
$1 < R < 5$ m	1.7	75 (dB)
$5 < R < 15$ m	1.7	65 (dB)
$15 < R < 30$ m	1.7	56 (dB)

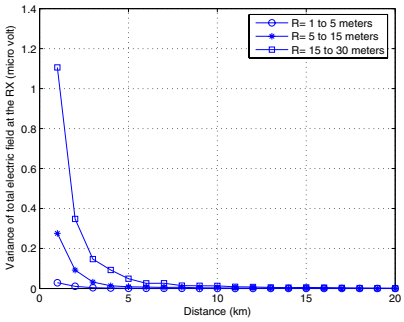

Figure 11. The variance of the total electric field at the RX versus distance for various radar cross sections

The variance of the total signal strength measured in terms of its electric field intensity versus the separation distance between the TX and the RX with the radar cross section as parameter is plotted in Fig. 11. It is evident that the variance decreases with the separation distance. This confirms the previous observation pertaining to the statistical regularity of the scattered signals arriving at the RX.

4) Effect of Ground Reflection

Finally the influence of the reflected signals due to the ground is investigated. The impact of ground reflection is studied via simulations for three different reflection mechanisms, which are characterized by $\Gamma_g = 1$, $\Gamma_g = 0$, and $\Gamma_g = -1$. Again 1000 simulation runs are performed for each value of the reflection coefficient. The other simulation parameters are set as follows: $N = 100$, the radar cross section radius $1 < R < 5$ m.

The simulation results are shown in the form of histograms for the path-loss exponents and its intercept values. Fig. 12, Fig. 13, and Fig. 14 show the histograms for $\Gamma_g = 1$, $\Gamma_g = -1$, and $\Gamma_g = 0$, respectively. The overall simulation results are

summarized in terms of the mean values and tabulated in Table II.

TABLE II. MEAN PATH LOSS EXPONENTS AND INTERCEPT VALUES FOR THREE DIFFERENT GROUND REFLECTION COEFFICIENTS

Ground Reflection	Mean Exponent	Mean Intercept
$\Gamma_g = 1$	1.18	75 (dB)
$\Gamma_g = 0$	1.42	76 (dB)
$\Gamma_g = -1$	1.7	75 (dB)

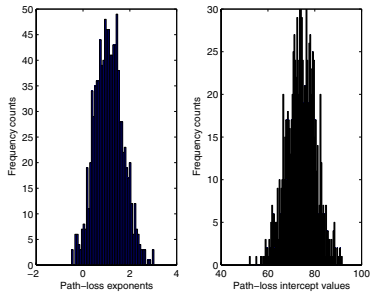

Figure 12. Histogram of path loss exponents and intercept values for $\Gamma_g = 1$ (mean exponent = 1.18; mean intercept = 75)

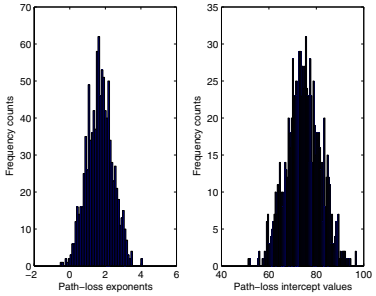

Figure 13. Histogram of path loss exponents and intercept values for $\Gamma_g = -1$ (mean exponent = 1.7; mean intercept = 75)

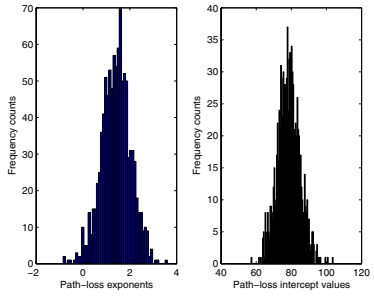

Figure 14. Histogram of path loss exponents and intercept values for $\Gamma_g = 0$ (mean exponent = 1.42; mean intercept = 76)

The simulation results are again consistent with physical facts. First, since the objects with radar cross section radius in the range $1 < R < 5$ m are small, the total received signals are weak. The path-loss intercept values are accordingly small. Hence, they tend to show little variation in the dB scale. Second, the likelihood of producing coherent signals are relatively high for $\Gamma_g = 1$, but relatively low for $\Gamma_g = -1$. And the likelihood falls in the middle when $\Gamma_g = 0$. Indeed, the corresponding path-loss exponents are 1.18, 1.7, and 1.42.

V. CONCLUSION

A ray tracing technique is proposed for the characterization of large-scale narrowband channels. No restrictive assumptions are made. This technique is especially suited for the study of path loss in wireless systems using computer simulations. The simulation results are in very good agreement with those obtained by experimental measurements with respect to the path-loss exponents and intercept values, such as the Hata model and the Lee model for macro cells. This computer simulation study leads to two key observations: First, the path loss is affected by the number of scattering objects, their radar cross sections, and the ground reflection. Second, coherent multipath signals can cause the path-loss exponent falling below 2, which corresponds to free-space propagation. It is also worthy pointing out that the advantages of computer modeling include low costs, flexibility, and universality in the sense that the derived model parameters are not site-specific. The proposed ray tracing model is flexible and may readily be adapted for other applications to channel modeling.

REFERENCES

[1] M. Hata, T. Nagatsu, "*Mobile location using signal strength measurement in cellular systems*," IEEE Trans. Veh. Tech., vol. 29, pp. 245-251, 1980.

[2] W. C. Y. Lee, "*Mobile Communications Design Fundamental*," Indianapolis, IN: Sams, 1986.

[3] Gordon L. Stüber, "*Principle of Mobile Communication,"* 2nd edition, Kluer Academic Publisher, 2001.

[4] H. R. Anderson, *"A ray-tracing propagation model for digital broadcast systems in urban area,"* IEEE Trans. Broadcasting, vol. 39, pp. 309-317, September 1993.

[5] J. W. McKown and R. L. Hamilton, Jr., *"Ray Tracing as a design tool for radio network,"* IEEE Network, pp. 27-30, November 1991.

[6] Andrea Goldsmiths, "*Wireless communications*," Cambridge University Press, 2005.

[7] T. S. Rappaport, "*Wireless Communications: Principles and Practice*," 2nd ed., Prentice Hall, 2002.

[8] K. R. Schaubach, N. J. Davis IV, T. S. Rappaport, *"A ray tracing method for predicting path loss and delay spread in microcellular environments*,*"* IEEE Veh. Trans. Tech., pp. 932-935, May 1992.

[9] H.-J. Li, C.-C. Chen, T.-Y. Liu, H.-C. Lin,"*Applicability of ray-tracing techniques for prediction of outdoor channel characteristics,*" IEEE Trans. Veh. Tech.; pp. 2336-2349, November 2000.

[10] A. Domazetovic, L. J. Greenstein, N. Mandayan, I. Seskar, "*A new modeling approach for wireless channels with predictable path geometries,*" IEEE Beh. Tech. Conf., September 2002.

[11] Hung Huy Khong, Bing W. Kwan, Leonard J. Tung, *"A Physics-Based Path-loss Model for UWB (Ultra Wide-Band) Systems,"*Proc. International Conference on Wireless Networks (ICWN) 2008, July 2008.

[12] Hung Huy Khong, Bing W. Kwan, Leonard J. Tung,"*Computer Simulation of Path Loss Using Ray Tracing,*" Internal Report (Submitted Conference Paper).

[13] Hung Huy Hung, "*Path Loss Model Based on Ray Tracing Technique,*" Master Thesis, Florida State University, Spring 2009.